This MICCAI paper is the Open Access version, provided by the MICCAI Society. It is identical to the accepted version, except for the format and this watermark; the final published version is available on SpringerLink.

Physical-Driven Unified Implicit Regularization Network with Scan Parameter Prompts for Accelerated Multi-parametric MR Imaging

Yan Yang[1,3], Han Xiao[1], Xue Yang[1], Jiazhen Wang[1(✉)], Sen Jia[2(✉)], Hairong Zheng[2], and Jian Sun[1]

[1] Xi'an Jiaotong University, Xi'an, China
[2] Shenzhen Institute of Advanced Technology, Shenzhen, China
[3] State Key Laboratory for Strength and Vibration of Mechanical Structures, Xi'an, China

{yangyan,jiansun}@xjtu.edu.cn, {hanx1121,xuey4123,jzwang}@stu.xjtu.edu.cn, {sen.jia,hr.zheng}@siat.ac.cn

Abstract. As an advanced MRI technique, multi-parametric magnetic resonance imaging provides valuable quantitative maps but necessitates long scan times. Accelerated imaging techniques are therefore essential, yet existing reconstruction methods often deliver suboptimal performance due to cascading errors between the reconstruction and quantification steps, and furthermore, lack adequate physical constraints on the signal model. To address these challenges, we propose a Physical-Driven Unified Implicit Regularization Network (PDUIR-Net) for joint estimation of images and quantitative maps in MRI. Specifically, the network is derived by unfolding the solver of an implicit-regularization reconstruction model with a unified objective. We further design a prompt-guided decoupled reconstruction module to disentangle shared and contrast-specific features across different contrasts, and develop a proximal quantitative mapping module to learn priors directly from data. Consequently, all components are integrated into an end-to-end trainable framework. Experimental results on our in-house data (12-echo sequence) show that our method outperforms the state-of-the-art methods by 1.18% in SSIM for multi-contrast images, and 0.89% in SSIM for quantitative maps at 10× acceleration, which significantly advances the performance limitation for multi-parametric MRI.

Keywords: Multi-parametric MRI · Fast MRI · Physics-Driven MRI

1 Introduction

Multi-parametric magnetic resonance imaging (MRI) is an advanced quantitative MRI technique that enables simultaneous acquisition of multiple intrinsic tissue properties (e.g., T_1 and T_2^*, and Proton Density maps) through a single scan, as exemplified by techniques such as MTP [9] and MRF [1], thereby facilitating quantitative clinical diagnosis of tumors, neurological disorders, and cardiovascular diseases [1–4, 9]. However, because acquiring multiple contrast images with varying flip angles (FAs), repetition times (TRs), and echo times (TEs) prolongs scan times, it is essential to develop a reconstruction method supporting accelerated multi-parametric MR imaging.

Multi-parametric MRI pipelines generally involve two stages, namely reconstructing multi-contrast images from undersampled k-space data and estimating multi-parametric maps using physical models. This workflow has given rise to two major lines of research: two-step approaches and one-step approaches. Two-step approaches reconstruct multi-contrast images first and then estimate multi-parametric maps separately [5–7]. For reconstruction, the field has progressed from single-contrast reconstruction [17, 23] to multi-contrast joint reconstruction [19], spanning iterative algorithms [23], deep networks [19, 18], and unrolled models [17]. For quantification, empirical physical models are often used for fitting, or deep learning is directly utilized for estimation. This line of work solves the two stages independently, which can lead to error propagation, and residual artifacts from the first stage ultimately result in suboptimal map estimation. In contrast, one-step methods employ integrated models to directly transform k-space data into parametric maps [12, 21, 22]. By jointly optimizing the reconstruction and quantification components, recent approaches such as MANTIS [13] and SRM-Net [14] have demonstrated significant performance gains. Furthermore, WDPM-Net [15] introduces multi-contrast feature interactions and physics-constrained mapping to enhance estimation accuracy. Despite these advances, the inherent objectives of image reconstruction and parameter quantification often remain imperfectly aligned. Consequently, naive joint optimization can lead to unstable training and reduced interpretability. This highlights the necessity of tightly coupling both processes through explicitly aligned physical constraints.

To this end, we introduce a novel Physical-Driven Unified Implicit Regularization Network (PDUIR-Net), designed to more effectively leverage MR physics to impose consistent constraints on image reconstruction and parameter estimation, thereby mitigating error propagation between these tasks. Specifically, we first formulate a unified model for joint estimation, incorporating three types of constraints, including data acquisition process, quantitative signal physics, and priors on both the images and the quantitative maps. To better capture two priors, we design a prompt-guided decoupled reconstruction module to disentangle shared and contrast-specific features across contrasts, and we develop a proximal quantitative mapping module. Together, these components constitute an implicit regularization scheme that learns the relevant priors from data. Finally, we unfold the resulting iterative optimization procedure into an end-to-end trainable network, enabling progressive joint estimation of the images and quantitative maps over successive iterations. In summary, **our contributions are mainly fourfold: (1)** We propose a new physics-driven deep network for joint estimation of images and quantitative maps in MRI. The network is derived by unfolding the solver of an implicit-regularization reconstruction model with a unified objective, which promotes objective consistency while improving interpretability.

(2) We use scan parameter as prompts to adaptively modulate prompt-guided decoupled reconstruction module, enabling effective disentanglement of shared and contrast-specific components across contrasts. This design reduces network parameters while improving reconstruction performance. **(3)** We learn a prior on signal ratios across multi-contrast images to indirectly model quantitative maps, transforming the original nonlinear constrained optimization into a linear constrained problem, which makes the model easier to solve and leads to more stable network training. **(4)** On our in-house dataset, our method yields improvements of 1.18% in SSIM for multi-contrast images, and 0.89% in SSIM for quantitative maps at 10× acceleration, thereby pushing the performance limits of multi-parametric MRI.

2 Method

2.1 Problem Formulation

In this work, we address accelerated multi-parametric MRI by embedding quantitative physical models into reconstruction pipeline, establishing a unified framework for joint estimation of multi-contrast images and quantitative maps. To better capture priors for both images and maps, we propose an implicit regularization approach using a deep network that learns shared–specific decoupled priors across contrasts and physics-informed priors for parameter maps. We then unroll the iterative optimization process of this model into an end-to-end trainable network that incorporates the underlying MRI physics and learnable priors.

Specifically, let $X = [x_1, x_2, ..., x_N] \in \mathbb{C}^{N\times D}$ be the complex-valued multi-contrast images to be reconstructed, where N is the number of contrasts and P is the number of pixels. The parameters R and S capture the signal evolution across different flip angles and repetition times, respectively. We propose the following unified physical-driven optimization model:

$$\hat{X}, \hat{S}, \hat{R} = \underset{X,S,R}{\arg\min} \left\{ \frac{1}{N} \sum_{i=1}^{N} \|Ax_i - y_i\|_2^2 + \mathcal{G}(X) + \lambda_3 \psi_3(f_S(X)) + \lambda_4 \psi_4(f_R(X)) \right\} \tag{1}$$

where A is the forward operator with the sampling mask, Fourier transform, and coil sensitivity, respectively; y_i represents the undersampled k-space data, and $\mathcal{G}(X)$ serves as the regularization term for joint reconstruction. The functions $f_S(X)$ and $f_R(X)$ denote the mapping of quantitative parameters. Directly optimizing this model is highly non-convex and unstable due to complex Bloch equations underlying quantitative maps. To address this, our innovation is to exploit the physical relationships defined by the signal ratios between multi-contrast images. According to [9], we define S as the signal ratio between adjacent echoes within the same repetition time (TR), and R as signal ratio between images acquired under different flip angles (FA). R and S are uniquely mapped to quantitative T_1 and T_2^* maps. For convenience, we also denote R and S as quantitative maps. Based on Multi-Dimensional Integration (MDI) theory [8],

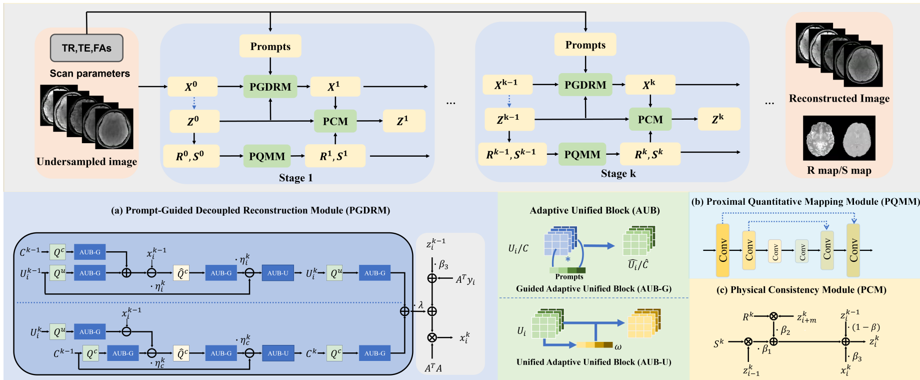

Fig. 1. The proposed PDUIR-Net integrates three dedicated modules: (a) the Prompt-Guided Decoupled Reconstruction Module (PGDRM), which performs image reconstruction; the Adaptive Unified Block (AUB) in PGDRM that refines the network; (b) the Proximal Quantitative Mapping Module (PQMM), responsible for estimating parameter maps; and (c) the Physical Consistency Module (PCM), which enforces contrast images by the physical constraint.

the estimation of these parameters relies on a weighted least-squares solution derived from nonlinear inter-image relationships. To convert these nonlinear relations into linear physical constraints, we employ the functions:

$$f_S(X) = \frac{1}{2}\sum_{i=1}^{T} \|x_i - x_{i-1} \odot S\|_2^2, \quad f_R(X) = \frac{1}{2}\sum_{i=1}^{P} \|x_i - x_{i+m} \odot R\|_2^2 \tag{2}$$

where T and P denote the number of image pairs utilized to compute S and R; m represents the index offset between different flip-angle groups, and $\odot$ denotes pixel-wise multiplication.

Since it is difficult to optimize X and R, S simultaneously in Eq. (1), we introduce an auxiliary variable Z to decouple the image reconstruction from the quantitative parameter estimation. By employing the Half-Quadratic Splitting (HQS) algorithm, the complex joint objective is decomposed into three tractable sub-problems. At the t-th iteration, the alternating steps are formulated as:

$$X^t = \arg\min_{X} \left\{ \lambda \sum_{i=1}^{N} \|Ax_i - y_i\|_2^2 + \mathcal{G}(X) + \frac{\beta_3}{2}\sum_{i=1}^{N} \left\|x_i - z_i^{t-1}\right\|_2^2 \right\} \tag{3a}$$

$$S^t, R^t = \arg\min_{S,R} \left\{ \phi_R(R) + \phi_S(S) + \frac{\beta_1}{2}\left\|f_R(Z^{t-1}) - R\right\|_2^2 + \frac{\beta_2}{2}\left\|f_S(Z^{t-1}) - S\right\|_2^2 \right\} \tag{3b}$$

$$Z^t = \arg\min_{Z} \left\{ \frac{\beta_1}{2}\left\|f_{R^t}(Z) - R^t\right\|_2^2 + \frac{\beta_2}{2}\left\|f_{S^t}(Z) - S^t\right\|_2^2 + \frac{\beta_3}{2}\sum_{i=1}^{N}\left\|x_i^t - z_i\right\|_2^2 \right\} \tag{3c}$$

2.2 Physical-Driven Unified Implicit Regularization Network

Derived by unrolling the alternating optimization algorithm for Eqn. (3), our proposed PDUIR-Net forms an end-to-end multi-stage architecture. As illustrated in Fig. 1, taking the undersampled image as input, PDUIR-Net jointly outputs the reconstructed multi-contrast images and the quantitative maps. Each stage consists of three key components: Prompt-Guided Decoupled Reconstruction Module, Proximal Quantitative Mapping Module, and Physical Consistency Module. Next, we will introduce these modules in detail.

Prompt-Guided Decoupled Reconstruction Module (PGDRM). This module is designed to update the multi-contrast images X in Eqn. (3a). Although multi-contrast images differ in signal intensity, they share consistent anatomical structures. Therefore, we introduce a convolutional dictionary model to decouple the images into common features C and unique features U_i:

$$x_i^t = Q_i^c \otimes C^t + Q_i^u \otimes U_i^t \tag{4}$$

where $\otimes$ denotes the convolutional operation, Q_i^c and Q_i^u are the common and unique filters, while C and U_i denote the common and unique features.

Plugging Eqn. (4) into sub-problem Eqn. (3a), the optimization problem can be decomposed into several proximal operators, yielding the iterative updates:

$$U_i^t = \mathrm{prox}_{\alpha_i \psi_i}\left(U_i^{t-1} - \eta_i^t \nabla \tilde{f}_i(U_i^{t-1})\right) \triangleq \mathrm{Net}_{U_i}\left(U_i^{t-1} - \eta_i^t \nabla \tilde{f}_i(U_i^{t-1})\right) \tag{5a}$$

$$C^t = \mathrm{prox}_{\alpha_c \psi_c}\left(C^{t-1} - \eta_c^t \nabla \tilde{g}(C^{t-1})\right) \triangleq \mathrm{Net}_{C}\left(C^{t-1} - \eta_c^t \nabla \tilde{g}(C^{t-1})\right) \tag{5b}$$

$$x_i^t = \left(A^T A + (\lambda + \beta_3) I\right)^{-1}\left(A^T y_i + \lambda(Q_i^c \otimes C^t + Q_i^u \otimes U_i^t) + \beta_3 z_i^{t-1}\right) \tag{5c}$$

where the gradients are given by($\otimes^T$ denotes the transposed convolution):

$$\nabla \tilde{f}_i(U_i^{t-1}) = Q_i^u \otimes^T \left(Q_i^c \otimes C^{t-1} + Q_i^u \otimes U_i^{t-1} - x_i^{t-1}\right) \tag{6a}$$

$$\nabla \tilde{g}(C^{t-1}) = \sum_{i=1}^{k} Q_i^c \otimes^T \left[Q_i^c \otimes C^{t-1} - \left(x_i^{t-1} - Q_i^u \otimes U_i^t\right)\right] \tag{6b}$$

To reduce the trainable parameters of PGDRM, we further design an **Adaptive Unified Block (AUB)**. Specifically, decoupling features across N distinct contrasts via Eqn. (4) conventionally requires N independent, contrast-specific sets of filters (Q_i^c, Q_i^u) alongside N separate update networks (Net_{U_i}) in Eqn. (5a). This results in significant redundancy and model complexity. To overcome this bottleneck, the AUB elegantly unifies the feature representation across all contrasts through two specialized sub-blocks:

(a) Guided Adaptive Unified Block (AUB-G). This sub-block targets the reduction of parameters in filters Q_i^c and Q_i^u. Its design is motivated by physical principles of multi-contrast images: images differences arise primarily from variations in scanning parameters (e.g., TR, TE, FA) as described by quantitative signal model. Therefore, AUB-G uses these scan parameters as conditioning prompts to identify image contrasts, allows a shared set of filters (Q^c, Q^u), dramatically cutting the parameter count. The process is formalized as:

$$x_i^t = Q^c \otimes \hat{C}^t + Q^u \otimes \hat{U}_i^t, \quad \hat{C}^t = C^t \,\mathrm{Linear}(P_i), \quad \hat{U}_i^t = U_i^t \,\mathrm{Linear}(P_i) \tag{7}$$

where P_i is an embedding code for the i-th contrast's unique scan parameters.

(b) Unified Adaptive Unified Block (AUB-U). This sub-block aims to further minimize parameters within the iterative network Net_{U_i} defined in Eqn. (5a). It replaces a sets of identical network Net_{U_i} with a content-aware adaptive refinement mechanism Net_U. This mechanism dynamically reweights the features U_i^t before a convolution, the refinement is performed as:

$$U_i^{t+1} = \mathrm{Net_u}\left(\omega_i \odot U_i^t\right), \quad \omega_i = \mathrm{Softmax}\left(\mathrm{Linear}\left(U_i^t\right)\right) \tag{8}$$

where ω_i represents self-learned attention weights derived from U_i^t themselves.

Proximal Quantitative Mapping Module (PQMM). This module is designed to update the quantitative maps R and S in Eqn.(3b). Instead of solving the proximal operators analytically, we extend this estimate to be a learnable module defined as:

$$R^t = \mathrm{prox}_{\frac{1}{\beta_1}\phi_R}\left(f_R(Z^{t-1})\right) \triangleq \mathrm{Net}_R(f_R(Z^{t-1})) \tag{9}$$

where Net_R employs U-Net architectures to directly estimate. S^t follows the same procedure as R^t.

Physical Consistency Module (PCM). This module solves Eqn. (3c) to update the auxiliary variable Z under the guidance of the estimated maps R and S. This step enforces physical consistency and provides feedback to the reconstruction network. Equation (3c) can be efficiently implemented via gradient descent:

$$z_i^t = (1-\beta)z_i^{t-1} + \beta_1(z_{i-1}^t \odot S^t) + \beta_2(z_{i+k}^t \odot R^t) + \beta_3 x_i^t \tag{10}$$

where $\beta = \beta_1 + \beta_2 + \beta_3$, with β_1, β_2, and β_3 being learnable hyperparameters for balancing different terms. k is the index offset for different flip-angle groups.

By connecting the modules of PGDRM, PQMM, and PCM alternately, we construct a physical-driven unified implicit regularization network (PDUIR-Net), as shown in Fig. 1.

2.3 Training Loss

The overall loss function in our framework consists of the multi-contrast reconstruction loss $\mathcal{L}_{\mathrm{Recon}}$ and the quantitative mapping loss $\mathcal{L}_{\mathrm{Map}}$, defined as:

$$\mathcal{L}_{\mathrm{total}} = \mathcal{L}_{\mathrm{Recon}} + \lambda_2 \mathcal{L}_{\mathrm{Map}} \tag{11}$$

where $\mathcal{L}_{\mathrm{Recon}} = \|X^K - X_{GT}\|_2 + \lambda_1 \mathcal{L}_{SSIM}(X^K - X_{GT})$ and $\mathcal{L}_{\mathrm{Map}} = \|R^K - R_{GT}\|_2 + \|S^K - S_{GT}\|_2$. K is the number of stages and empirically set to 4. The hyperparameters λ_1 and λ_2 balance the different losses and are empirically set to 0.5 and 0.01, respectively.

Table 1. Quantitative comparison of performance under different acceleration factors

AF	Method	Reconstruction			T1			T2*		
		SSIM	PSNR	NRMSE	SSIM	PSNR	NRMSE	SSIM	PSNR	NRMSE
6×	TV	0.889	35.65	0.078	0.944	28.30	0.116	0.919	27.66	0.077
	SRM-Net	0.770	21.42	0.449	0.878	23.18	0.211	0.791	19.01	0.228
	MTrans	0.841	27.36	0.204	0.837	22.50	0.225	0.800	20.06	0.193
	MD-GFormer	0.946	35.30	0.082	0.947	27.67	0.125	0.924	26.81	0.088
	MC-CDic	0.950	38.46	0.063	0.959	29.52	0.102	0.946	29.40	0.068
	Ours	**0.957**	**38.47**	**0.058**	**0.959**	**29.57**	**0.101**	**0.947**	**29.48**	**0.067**
10×	TV	0.855	32.90	0.109	0.925	26.76	0.139	0.886	25.80	0.259
	SRM-Net	0.753	21.06	0.458	0.870	23.60	0.201	0.768	18.65	0.615
	MTrans	0.827	26.79	0.222	0.832	22.59	0.222	0.801	20.92	0.452
	MD-GFormer	0.926	33.32	0.103	0.924	26.20	0.148	0.903	26.44	0.239
	MC-CDic	0.934	34.51	0.093	0.934	27.37	0.130	0.916	27.35	0.216
	Ours	**0.946**	**36.47**	**0.072**	**0.941**	**27.89**	**0.123**	**0.927**	**28.24**	**0.195**

3 Experiments

Dataset and Implementation Details. We evaluated our model on an in-house complex-valued dataset acquired by MULTIPLEX (MTP) based on a 3T scanner (uMR 790). The MTP is a gradient echo pulse sequence (GRE) with following scanning parameters: $FA_1/FA_2 = 4°/16°$, $TR_1/TR_2 = 44.5$ms, and six echo images per FA with TR_1 (TE = 4.01 ms) and TR_2 (TE = 4.01/10.29/16.57/22.85/29.13 ms). Specifically, our dataset includes 33 subjects, with 12 echos per subject. The MRI scanning was based on a 32-channel head coil with a voxel size of $0.68 \times 0.68 \times 2\,\text{mm}^3$ and slice matrix size of $336 \times 288 \times 84$. To match the actual sampling conditions, we need to perform undersampling on the ky-kz (288×84) plane with poisson-disc sampling masks at acceleration factors (AF) of 6× and 10×. Our model inputs the coil-combined data using sensitivity maps calculated by ESPIRiT [16]. We randomly divided the 33 subjects into 24, 4 and 5 for training, validation, and testing, corresponding to 7260, 5280, and 880 slices, respectively. Quantitative evaluation metrics included NRMSE, SSIM, and PSNR. All our experiments were based on two NVIDIA A6000 GPUs (with 40 GB RAM) and the PyTorch framework. Moreover, we applied the Adam optimizer and trained the model for 100 epochs with mini-batch size set to 2 and learning rate set to 1×10^{-4}. The code is available at https://github.com/xjtuMIMILAB/PDUIR-Net.

Comparison with State-of-the-Art Methods. We compare the proposed approach against the traditional Total Variation (TV) method [23], multi-contrast MRI reconstruction methods (MTrans [18], MD-GFormer [19] and MC-CDic [20]), and representative quantitative MRI reconstruction method SRM-Net [14]. The quantitative comparison with the existing SOTA methods is summarized in Table 1, where our PDUIR-Net consistently presents promising NRMSE, SSIM and PSNR under varied accelerating factors. The qualitative comparison as illustrated in Fig. 2, our reconstructed images contain more detailed and clearer tissue structures than compared methods.

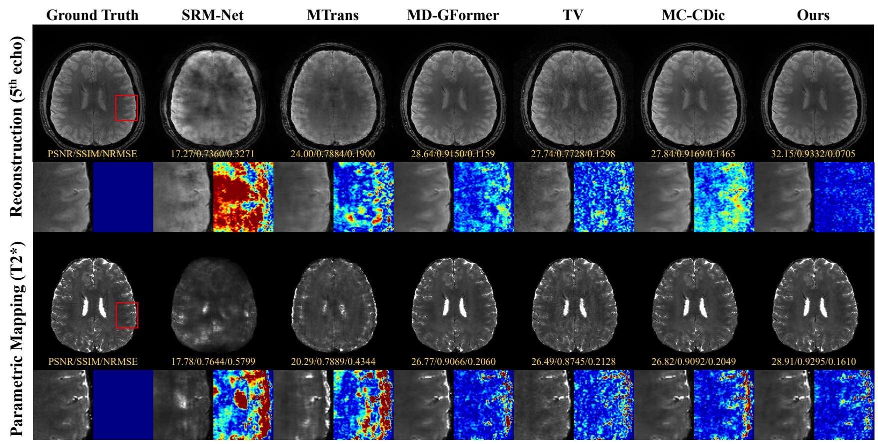

Fig. 2. Visual comparison of different methods on the test data with 10× Poisson-disc sampling. The red boxes indicate regions shown in close up views.

Table 2. Ablation study for three main components of our PDUIR-Net, including the Unified Adaptive Unified Block (AUB-U),Guided Adaptive Unified Block (AUB-G), and Physical Consistency Module (PCM).

AUB-U	AUB-G	PCM	Reconstruction			T1 Mapping			T2 Mapping		
			SSIM	PSNR	NRMSE	SSIM	PSNR	NRMSE	SSIM	PSNR	NRMSE
			0.930	33.54	0.106	0.934	27.25	0.132	0.916	27.35	0.216
✓			0.934	34.51	0.093	0.937	27.27	0.130	0.919	27.41	0.215
✓	✓		0.937	35.72	0.080	0.941	27.68	0.126	0.927	28.16	0.197
✓	✓	✓	**0.946**	**36.47**	**0.072**	**0.943**	**27.89**	**0.123**	**0.928**	**28.24**	**0.195**

Ablation Study. We conduct ablation experiments under 10× acceleration to evaluate the effectiveness of the main components in PDUIR-Net, as shown in Table 2. Row 4 denotes the full model. Removing PCM in Row 3 leads to degraded performance in both reconstruction and quantitative mapping, indicating the importance of physical consistency. Further removing AUB-G in Row 2 reduces the benefit of scan-parameter-guided adaptive filtering. Row 1 removes AUB-U and uses separate update networks, resulting in the weakest performance. The full model achieves the best results across all metrics, showing that AUB-U, AUB-G, and PCM jointly improve the reconstruction and mapping accuracy.

4 Conculsion

In this paper, we propose a novel Physical-Driven Unified Implicit Regularization Network (PDUIR-Net) for accelerated multi-parametric MRI. First, a unified joint estimation model is formulated, integrating three key constraints: the data acquisition process, the quantitative signal physics, and prior knowledge of both contrast images and parameter maps. To effectively capture priors, we introduce a prompt-guided decoupled reconstruction module that disentangles features into shared and contrast-specific components with scan-parameter guided and develop a proximal quantitative mapping module. These components are integrated to learn relevant priors directly from data. Finally,the resulting iterative optimization procedure is unfolded into an end-to-end trainable network that executes over successive stages. Experimental validation on an in-house 12-echo dataset shows that PDUIR-Net achieves superior performance over state-of-the-art methods in both reconstruction quality and quantitative mapping accuracy, demonstrating its effectiveness for accelerated multi-parametric MRI.

Acknowledgments. This work was practically supported by the National Natural Science Foundation of China (12401671, 12526209, 62301548, 62125111), Postdoctoral Research Funding of Shaanxi Province (2024BSHTDZZ007), Natural Science Foundation of Guangdong Province (2025A1515010915).

Disclosure of Interests. The authors have no competing interests to declare that are relevant to the content of this article.

References

1. Ma, D., Gulani, V., Seiberlich, N., Liu, K., Sunshine, J.L., Duerk, J.L., Griswold, M.A.: Magnetic resonance fingerprinting. Nature. **495**(7440), 187–192 (2013).
2. Cheng, H.-L.M., Wright, G.A.: Rapid high-resolution T1 mapping by variable flip angles: Accurate and precise measurements in the presence of radiofrequency field inhomogeneity. Magn. Reson. Med. **55**(3), 566–574 (2006).
3. Welsch, G.H., Hennig, F.F., Krinner, S., Trattnig, S.: T2 and T2* mapping. Curr. Radiol. Rep. **2**(8), 60 (2014).
4. Cordes, D., Yang, Z., Zhuang, X., Sreenivasan, K., Mishra, V., Hua, L.H.: A new algebraic method for quantitative proton density mapping using multi-channel coil data. Med. Image Anal. **40**, 154–171 (2017).
5. Chen, E.Z., et al.: Accelerating 3D MULTIPLEX MRI reconstruction with deep learning. In: Proceedings of the 29th Annual Meeting of the International Society for Magnetic Resonance in Medicine (2021).
6. Zhang, C., et al.: A unified model for reconstruction and R2* mapping of accelerated 7T data using the quantitative recurrent inference machine. NeuroImage. **264**, 119680 (2022).
7. Zibetti, M.V.W., et al.: Comparing learned variational networks and compressed sensing for $T_{1\rho}$ mapping of knee cartilage. Presented at the ISMRM Workshop on Machine Learning, Part II (2018).
8. Ye, Y., Lyu, J., Sun, W., et al.: A multi-dimensional integration (MDI) strategy for MR T2* mapping. NMR in Biomedicine. **34**(7), p. e4529 (2021).
9. Ye, Y., Lyu, J., Hu, Y., Zhang, Z., Xu, J., Zhang, W.: MULTI-parametric MR imaging with fLEXible design (MULTIPLEX). Magn. Reson. Med. **87**(2), 658–673 (2022).
10. Block, K.T., Uecker, M., Frahm, J.: Model-based iterative reconstruction for radial fast spin-echo MRI. IEEE Trans. Med. Imaging. **28**(11), 1759–1769 (2009).

11. Cai, C., et al.: Single-shot T2 mapping using overlapping-echo detachment planar imaging and a deep convolutional neural network. Magn. Reson. Med. **80**(5), 2202–2214 (2018).
12. Jun, Y., et al.: Deep model-based magnetic resonance parameter mapping network (dopamine) for fast T1 mapping using variable flip angle method. Med. Image Anal. **70**, 102017 (2021).
13. Liu, F., Feng, L., Kijowski, R.: Mantis: Model-augmented neural network with incoherent k-space sampling for efficient MR parameter mapping. Magn. Reson. Med. **82**(1), 174–188 (2019).
14. Liu, Y., Sun, K., Qi, H., et al.: SRM-Net: Joint sampling and reconstruction and mapping network for accelerated 3T brain multi-parametric MR imaging. IEEE Trans. Biomed. Eng. **72**(6), 1811–1824 (2025).
15. Dan, R., Sun, K., Zhou, Y., Jia, M., Liu, Y., Zhang, H., Zong, X., Shen, D.: Wavelet-driven decoupling and physics-informed mapping network for accelerated multi-parametric MR imaging. In International Conference on Medical Image Computing and Computer-Assisted Intervention, pp. 661–671(2025).
16. Uecker, M., et al.: Espirit—an eigenvalue approach to autocalibrating parallel MRI: Where sense meets grappa. Magn. Reson. Med. **71**(3), 990–1001 (2014).
17. Yang,Y., Sun, J., Li, H., Xu, Z.: Deep ADMM-Net for compressive sensing MRI. In: Advances in Neural Information Processing Systems,10-18 (2016).
18. Feng, C.-M., Yan, Y., Chen, G., Xu, Y., Hu, Y., Shao, L., Fu, H.: Multimodal transformer for accelerated MR imaging. IEEE Trans. Med. Imaging. **42**(10), 2804–2816 (2023).
19. Wang, J., Yang, Y., Yang, H., et al.: MD-GraphFormer: A model-driven graph transformer for fast multi-contrast MR imaging. IEEE Trans. Comput. Imaging. **9**, 1018–1030 (2023).
20. Lei, P., Zhang, M., Fang, F., Zhang, G.: Robust deep convolutional dictionary model with alignment assistance for multi-contrast MRI super-resolution. IEEE Trans. Med. Imaging. **44**(8), 3383–3396 (2025).
21. Dikaios, N., Arridge, S., Hamy, V., et al.: Direct parametric reconstruction from undersampled (k, t)-space data in dynamic contrast enhanced MRI. Med. Image Anal. **18**(7), 989–1001 (2014).
22. Zhou, Y., Wang, H., Liu, Y., Liang, D., Ying, L.: Accelerating MR parameter mapping using nonlinear compressive manifold learning and regularized pre-imaging. IEEE Trans. Biomed. Eng. **69**(10), 2996–3007 (2022).
23. Lustig, M., Donoho, D., Pauly, J.M.: Sparse MRI: The application of compressed sensing for rapid MR imaging. Magn. Reson. Med. **58**(6), 1182–1195 (2007).
24. Li, J., Yang, H., Yi, Q., Lu, M., Shi, J., Zeng, T.: High-frequency modulated transformer for multi-contrast MRI super-resolution. IEEE Trans. Med. Imaging. **44**(7), 3089–3099 (2025).